Pion-kaon Form Factors at High Precision

B. Ananthanarayan

Centre for High Energy Physics, Indian Institute of Science,
Bangalore 560 012, India

Seminar

IPN Orsay

June 17, 2010

Outline

- The process and definitions

Outline

- The process and definitions
- Status of experimental information and inputs

Outline

- The process and definitions
- Status of experimental information and inputs
- QCD correlators and dispersion relations

Outline

- The process and definitions
- Status of experimental information and inputs
- QCD correlators and dispersion relations
- Conformal methods and constraints

Outline

- The process and definitions
- Status of experimental information and inputs
- QCD correlators and dispersion relations
- Conformal methods and constraints
- Results and discussion

Outline

- The process and definitions
- Status of experimental information and inputs
- QCD correlators and dispersion relations
- Conformal methods and constraints
- Results and discussion
- Based on the papers:
  Gauhar Abbas and BA, European Physical Journal A 41 (2009) 7.
  Gauhar Abbas, BA, I. Caprini, I. Sentitemsu Imsong and S. Ramanan, European Physical Journal A 44 (2010) 175.
  Gauhar Abbas, BA, I. Caprini, I. Sentitemsu Imsong and S. Ramanan, arXiv: 1004.4257

Process and Definitions

- The semi-leptonic decays are the processes $K \to \pi l \nu_l$ (and $\tau \to \pi K \nu_\tau$).

Process and Definitions

- The semi-leptonic decays are the processes $K \to \pi l \nu_l$ (and $\tau \to \pi K \nu_\tau$).
- The matrix element for K^+_{l3} has the structure:

$$T = \frac{G_F}{\sqrt{2}} V^*_{us} l^\mu F^+_\mu(p', p)$$

$$l^\mu = \overline{u}(p_\nu)\gamma^\mu(1-\gamma_5)v(p_l)$$

$$F^+(p', p)_\mu = \langle \pi^0(p')|\bar{s}\gamma_\mu u|K^+(p)\rangle = \frac{1}{\sqrt{2}}((p'+p)_\mu f_+(t) + (p-p')_\mu f_-(t))$$

Process and Definitions

- The semi-leptonic decays are the processes $K \to \pi l \nu_l$ (and $\tau \to \pi K \nu_\tau$).
- The matrix element for K^+_{l3} has the structure:

$$T = \frac{G_F}{\sqrt{2}} V^*_{us} l^\mu F^+_\mu(p', p)$$

$$l^\mu = \overline{u}(p_\nu)\gamma^\mu(1-\gamma_5)v(p_l)$$

$$F^+(p', p)_\mu = \langle \pi^0(p')|\bar{s}\gamma_\mu u|K^+(p)\rangle = \frac{1}{\sqrt{2}}((p'+p)_\mu f_+(t) + (p-p')_\mu f_-(t))$$

- Neutral $F^0_\mu(p', p)$ defined without the $1/\sqrt{2}$
  Recent review for isospin violation, A. Kastner and H. Neufeld, European Physical Journal C57 (2008) 541.

Process and Definitions

- The semi-leptonic decays are the processes $K \to \pi l \nu_l$ (and $\tau \to \pi K \nu_\tau$).
- The matrix element for K^+_{l3} has the structure:

$$T = \frac{G_F}{\sqrt{2}} V^*_{us} l^\mu F^+_\mu(p', p)$$

$$l^\mu = \overline{u}(p_\nu)\gamma^\mu(1-\gamma_5)v(p_l)$$

$$F^+(p', p)_\mu = \langle \pi^0(p')|\overline{s}\gamma_\mu u|K^+(p)\rangle = \frac{1}{\sqrt{2}}((p'+p)_\mu f_+(t) + (p-p')_\mu f_-(t))$$

- Neutral $F^0_\mu(p', p)$ defined without the $1/\sqrt{2}$
  Recent review for isospin violation, A. Kastner and H. Neufeld, European Physical Journal C57 (2008) 541.
- $f_+(t), t = (p'-p)^2$ is known as the vector form factor as it is the P-wave projection of the crossed channel matrix element $\langle 0|\overline{s}\gamma_\mu u|K^+\pi^0, \text{in}\rangle$.

Definitions continued

- The scalar form factor

$$f_0(t) = f_+(t) + \frac{t}{M_K^2 - M_\pi^2} f_-(t)$$

is the analogous S-wave projection

Definitions continued

- The scalar form factor

$$f_0(t) = f_+(t) + \frac{t}{M_K^2 - M_\pi^2} f_-(t)$$

  is the analogous S-wave projection
- The physical region is $m_l^2 \leq t \leq (M_K - M_\pi)^2$ where the form factor is real

Definitions continued

- The scalar form factor

$$f_0(t) = f_+(t) + \frac{t}{M_K^2 - M_\pi^2} f_-(t)$$

is the analogous S-wave projection

- The physical region is $m_l^2 \leq t \leq (M_K - M_\pi)^2$ where the form factor is real
- Consider the expansion about $t = 0$

$$f_0(t) = f_+(0) \left(1 + \lambda_0' \frac{t}{M_\pi^2} + \frac{1}{2}\lambda_0'' \frac{t^2}{M_\pi^4} + \cdots \right),$$

$\lambda_0' = M_\pi^2 \langle r_{\pi\mathrm{K}}^2 \rangle / 6$, $\lambda_0'' = 2M_\pi^4\, c$ are related to the radius $\langle r_{\pi\mathrm{K}}^2 \rangle$ and curvature c used alternatively in the literature.

Definitions continued

- The scalar form factor

$$f_0(t) = f_+(t) + \frac{t}{M_K^2 - M_\pi^2} f_-(t)$$

  is the analogous S-wave projection

- The physical region is $m_l^2 \leq t \leq (M_K - M_\pi)^2$ where the form factor is real
- Consider the expansion about $t = 0$

$$f_0(t) = f_+(0)\left(1 + \lambda_0' \frac{t}{M_\pi^2} + \frac{1}{2}\lambda_0'' \frac{t^2}{M_\pi^4} + \cdots\right),$$

  $\lambda_0' = M_\pi^2 \langle r_{\pi \mathrm{K}}^2 \rangle / 6$, $\lambda_0'' = 2M_\pi^4 \, c$ are related to the radius $\langle r_{\pi \mathrm{K}}^2 \rangle$ and curvature c used alternatively in the literature.

- Analogously defined the vector form factor.

Sources of information

- The value $f_+(0)$ comes from theory.

Sources of information

- The value $f_+(0)$ comes from theory.
- Chiral theorems for the scalar form factors which are related to F_π/F_K.

Sources of information

- The value $f_+(0)$ comes from theory.
- Chiral theorems for the scalar form factors which are related to F_π/F_K.
- The slope and curvature parameters are determined from fitting to Dalitz plot distributions. Detailed discussion on experiments will be presented.

Sources of information

- The value $f_+(0)$ comes from theory.
- Chiral theorems for the scalar form factors which are related to F_π/F_K.
- The slope and curvature parameters are determined from fitting to Dalitz plot distributions. Detailed discussion on experiments will be presented.
- More recently from τ decays. BELLE has fitted them with resonances in the time-like region on the unitarity cut.

Sources of information

- The value $f_+(0)$ comes from theory.
- Chiral theorems for the scalar form factors which are related to F_π/F_K.
- The slope and curvature parameters are determined from fitting to Dalitz plot distributions. Detailed discussion on experiments will be presented.
- More recently from τ decays. BELLE has fitted them with resonances in the time-like region on the unitarity cut.
- Solutions of Muskelishvili-Omnès equations for form factors using phase shift information and some additional inputs to self- consistently generate them. Work of Moussallam, group of Jamin, Oller, Pich, Boito, Escribano.

$f_+(0)$

- $f_+(0) = 1$ in the limit of $m_d = m_u = m_s = 0$ ($SU(3)$ limit where all the eight pseudoscalars are Goldstone particles).

$f_+(0)$

- $f_+(0) = 1$ in the limit of $m_d = m_u = m_s = 0$ ($SU(3)$ limit where all the eight pseudoscalars are Goldstone particles).
- Corrections to the relation due to $SU(3)$ breaking. Expected to depart by $\sim 20\%$.

$f_+(0)$

- $f_+(0) = 1$ in the limit of $m_d = m_u = m_s = 0$ ($SU(3)$ limit where all the eight pseudoscalars are Goldstone particles).
- Corrections to the relation due to $SU(3)$ breaking. Expected to depart by $\sim 20\%$.
- Even smaller due to Ademollo-Gatto theorem.

$f_+(0)$

- $f_+(0) = 1$ in the limit of $m_d = m_u = m_s = 0$ ($SU(3)$ limit where all the eight pseudoscalars are Goldstone particles).
- Corrections to the relation due to $SU(3)$ breaking. Expected to depart by $\sim 20\%$.
- Even smaller due to Ademollo-Gatto theorem.
- Crucial for knowledge of Cabibbo-Kobayashi-Maskawa matrix as the combination $f_+(0)V_{us}$ appears in the expression for rates and Dalitz plot densities.

$f_+(0)$

- $f_+(0) = 1$ in the limit of $m_d = m_u = m_s = 0$ ($SU(3)$ limit where all the eight pseudoscalars are Goldstone particles).
- Corrections to the relation due to $SU(3)$ breaking. Expected to depart by $\sim 20\%$.
- Even smaller due to Ademollo-Gatto theorem.
- Crucial for knowledge of Cabibbo-Kobayashi-Maskawa matrix as the combination $f_+(0)V_{us}$ appears in the expression for rates and Dalitz plot densities.
- Crucial work by H. Leutwyler and M. Roos, Zeitschrift für Physik, C25 (1984) 91.

$f_+(0)$

- $f_+(0) = 1$ in the limit of $m_d = m_u = m_s = 0$ ($SU(3)$ limit where all the eight pseudoscalars are Goldstone particles).
- Corrections to the relation due to $SU(3)$ breaking. Expected to depart by $\sim 20\%$.
- Even smaller due to Ademollo-Gatto theorem.
- Crucial for knowledge of Cabibbo-Kobayashi-Maskawa matrix as the combination $f_+(0)V_{us}$ appears in the expression for rates and Dalitz plot densities.
- Crucial work by H. Leutwyler and M. Roos, Zeitschrift für Physik, C25 (1984) 91.
- Recent determinations from the lattice, e.g., RBC+UKQCD collaboration [P. A. Boyle et al., Physical Review Letters 100 (2008) 141601] gives $f_+(0) = 0.964(5)$. They use 2+1 flavour of dynamical wall quarks.

Low energy theorems, F_K/F_π - I

- A soft-pion theorem due to Callan and Treiman (C. G. Callan and S. B. Treiman, Physical Review Letters 16 (1966) 153) says

$$f_0(M_K^2 - M_\pi^2) = F_K/F_\pi + \Delta_{CT}$$

$\Delta_{CT} \simeq 0$ to two-loops in chiral perturbation theory (J. Bijnens and P. Talavera, Nuclear Physics B 669 (2003) 341.)
This point called CT_1 is above the end-point of the K_{l3} but is in the analyticity part of the timelike region.

Low energy theorems, F_K/F_π - I

- A soft-pion theorem due to Callan and Treiman (C. G. Callan and S. B. Treiman, Physical Review Letters 16 (1966) 153) says

$$f_0(M_K^2 - M_\pi^2) = F_K/F_\pi + \Delta_{CT}$$

  $\Delta_{CT} \simeq 0$ to two-loops in chiral perturbation theory (J. Bijnens and P. Talavera, Nuclear Physics B 669 (2003) 341.)
  This point called CT_1 is above the end-point of the K_{l3} but is in the analyticity part of the timelike region.
- Knowledge of F_K/F_π at high precision is therefore crucial.

Low energy theorems, F_K/F_π - II

- A soft-kaon theorem due to Oehme (R. Oehme, Physical Review Letters 16 (1966) 215) says

$$f_0(M_\pi^2 - M_K^2) = F_\pi/F_K + \overline{\Delta}_{CT}$$

$\overline{\Delta}_{CT} = 0.03$ is one-loop in chiral perturbation theory (J. Gasser and H. Leutwyler, Nuclear Physics B250 (1985) 517).
This point known as CT_2 is in the spacelike region.

Low energy theorems, F_K/F_π - III

- No such relations for vector form factor.

Low energy theorems, F_K/F_π - III

- No such relations for vector form factor.
- As a result, scalar form factor much better suited to theoretical analysis.

Low energy theorems, F_K/F_π - III

- No such relations for vector form factor.
- As a result, scalar form factor much better suited to theoretical analysis.
- These relations in the unphysical region will be used by us in the unitarity bound technique.

Low energy theorems, F_K/F_π - III

- No such relations for vector form factor.
- As a result, scalar form factor much better suited to theoretical analysis.
- These relations in the unphysical region will be used by us in the unitarity bound technique.
- $F_K/F_\pi = 1.193 \pm 0.006$ according to recent lattice evaluations (see e.g., L. Lellouch, arXiv:0902.4545; see also A. Bazavov et al. [MILC collaboration], arXiv:0910.2966, which uses 2+1 flavor with improved staggered quark action). Confirmed by S. Dürr et al. [BMW collaboration], arXiv:1001.4692.

Low energy theorems, F_K/F_π - III

- No such relations for vector form factor.
- As a result, scalar form factor much better suited to theoretical analysis.
- These relations in the unphysical region will be used by us in the unitarity bound technique.
- $F_K/F_\pi = 1.193 \pm 0.006$ according to recent lattice evaluations (see e.g., L. Lellouch, arXiv:0902.4545; see also A. Bazavov et al. [MILC collaboration], arXiv:0910.2966, which uses 2+1 flavor with improved staggered quark action). Confirmed by S. Dürr et al. [BMW collaboration], arXiv:1001.4692.
- An extremely interesting joint analysis of $f_+(0)$ and F_K/F_π is by V. Bernard and E. Passemar, arXiv:0912.3792

Information circa 1994

- Important review is the article by J. Bijnens, G. Colangelo and J. Gasser in the DAFNE Handbook on Leptonic and Semileptonic Kaon Decays.

Information circa 1994

- Important review is the article by J. Bijnens, G. Colangelo and J. Gasser in the DAFNE Handbook on Leptonic and Semileptonic Kaon Decays.
- Charged kaon decays with electron: $\lambda_+ = 0.028 \pm 0.004$
  Neutron kaon decays with electron: $\lambda_+ = 0.030 \pm 0.0016$
  (Note also that there was no prime on the symbols at that time.)
  (Comment: no information on scalar form factor. Kinematically suppressed.)

Information circa 1994

- Important review is the article by J. Bijnens, G. Colangelo and J. Gasser in the DAFNE Handbook on Leptonic and Semileptonic Kaon Decays.
- Charged kaon decays with electron: $\lambda_+ = 0.028 \pm 0.004$
  Neutron kaon decays with electron: $\lambda_+ = 0.030 \pm 0.0016$
  (Note also that there was no prime on the symbols at that time.)
  (Comment: no information on scalar form factor. Kinematically suppressed.)
- Neutral kaon decays with muon: $\lambda_+ = 0.030 \pm 0.003,\ \lambda_0 = 0.019 \pm 0.004$ from SLAC based on 1.6 million K_L decays.
  Look into the handbook for more comments and status, and also on charged kaon into muon decays.

Information circa 1994

- Important review is the article by J. Bijnens, G. Colangelo and J. Gasser in the DAFNE Handbook on Leptonic and Semileptonic Kaon Decays.
- Charged kaon decays with electron: $\lambda_+ = 0.028 \pm 0.004$
  Neutron kaon decays with electron: $\lambda_+ = 0.030 \pm 0.0016$
  (Note also that there was no prime on the symbols at that time.)
  (Comment: no information on scalar form factor. Kinematically suppressed.)
- Neutral kaon decays with muon: $\lambda_+ = 0.030 \pm 0.003,\ \lambda_0 = 0.019 \pm 0.004$ from SLAC based on 1.6 million K_L decays.
  Look into the handbook for more comments and status, and also on charged kaon into muon decays.
- The same article gives at one-loop in chiral perturbation theory $0.031,\ 0.017 \pm 0.004$ respectively

Information circa 1994

- Important review is the article by J. Bijnens, G. Colangelo and J. Gasser in the DAFNE Handbook on Leptonic and Semileptonic Kaon Decays.
- Charged kaon decays with electron: $\lambda_+ = 0.028 \pm 0.004$
  Neutron kaon decays with electron: $\lambda_+ = 0.030 \pm 0.0016$
  (Note also that there was no prime on the symbols at that time.)
  (Comment: no information on scalar form factor. Kinematically suppressed.)
- Neutral kaon decays with muon: $\lambda_+ = 0.030 \pm 0.003,\ \lambda_0 = 0.019 \pm 0.004$ from SLAC based on 1.6 million K_L decays.
  Look into the handbook for more comments and status, and also on charged kaon into muon decays.
- The same article gives at one-loop in chiral perturbation theory $0.031,\ 0.017 \pm 0.004$ respectively
- **(Note: no mention of curvature parameters which was the state of the art at that time)**

ISTRA experiment

- Experimental setup up at the IHEP 70 GeV proton synchrotron U-70. Secondary beam with about 25 GeV protons. Analysis is based on Dalitz plot density.

ISTRA experiment

- Experimental setup up at the IHEP 70 GeV proton synchrotron U-70. Secondary beam with about 25 GeV protons. Analysis is based on Dalitz plot density.
- O. P. Yushchenko et al., Physics Letters B 581 (2004) 31. Charged kaon to muon mode.
  $\lambda_+ = 0.0277 \pm 0.0013(\mathrm{stat}) \pm 0.0009(\mathrm{syst})$
  $\lambda_0 = 0.0183 \pm 0.0011(\mathrm{stat}) \pm 0.0006(\mathrm{syst})$
  based on 540,000 events.
  (No curvature assumed.)

ISTRA experiment

- Experimental setup up at the IHEP 70 GeV proton synchrotron U-70. Secondary beam with about 25 GeV protons. Analysis is based on Dalitz plot density.
- O. P. Yushchenko et al., Physics Letters B 581 (2004) 31. Charged kaon to muon mode.
  $\lambda_+ = 0.0277 \pm 0.0013(\text{stat}) \pm 0.0009(\text{syst})$
  $\lambda_0 = 0.0183 \pm 0.0011(\text{stat}) \pm 0.0006(\text{syst})$
  based on 540,000 events.
  (No curvature assumed.)
- O. P. Yushchenko et al., Physics Letters B 589 (2004) 111. Charged kaon to electron mode.
  Curvature assumed here for vector form factor but scalar slope not reported.
  based on 540,000 events.

KLOE experiment

- KLOE detector at DAFNE (e^+e^- collider at 1.02 GeV)

KLOE experiment

- KLOE detector at DAFNE (e^+e^- collider at 1.02 GeV)
- $K_L \to \pi\mu\nu$ analysis based on about 1.8 million events from 328 pb^{-1} of data.

KLOE experiment

- KLOE detector at DAFNE (e^+e^- collider at 1.02 GeV)
- $K_L \to \pi\mu\nu$ analysis based on about 1.8 million events from 328 pb^{-1} of data.
- F. Ambrosino et al., JHEP 0712 (2007) 105. Report only slope parameters for vector and scalar to be $(25.7 \pm 0.6) \times 10^{-3}$ and $(14.0 \pm 2.1) \times 10^{-3}$ respectively.

NA48 experiment

- K_L produced at the 450 GeV SPS proton synchrotron at CERN.

NA48 experiment

- K_L produced at the 450 GeV SPS proton synchrotron at CERN.
- A. Lai et al., Physics Letters B 602 (2004) 41, electron mode.
  Do not report slope, but reports $V_{us} f_+(0)$

NA48 experiment

- K_L produced at the 450 GeV SPS proton synchrotron at CERN.
- A. Lai et al., Physics Letters B 602 (2004) 41, electron mode.
  Do not report slope, but reports $V_{us} f_+(0)$
- A. Lai et al., Physics Letters B 647 (2007) 341, muon mode

NA48 experiment

- K_L produced at the 450 GeV SPS proton synchrotron at CERN.
- A. Lai et al., Physics Letters B 602 (2004) 41, electron mode.
  Do not report slope, but reports $V_{us} f_+(0)$
- A. Lai et al., Physics Letters B 647 (2007) 341, muon mode
- No curvature found for the scalar!

NA48 experiment

- K_L produced at the 450 GeV SPS proton synchrotron at CERN.
- A. Lai et al., Physics Letters B 602 (2004) 41, electron mode.
  Do not report slope, but reports $V_{us}f_+(0)$
- A. Lai et al., Physics Letters B 647 (2007) 341, muon mode
- No curvature found for the scalar!
- Possibly controversial.

KTeV experiment

- KTeV experiment at Fermilab. 1.9 million K_L electron and 1.5 million K_L muono decays.

KTeV experiment

- KTeV experiment at Fermilab. 1.9 million K_L electron and 1.5 million K_L muono decays.
- T. Alexopoulos et al., Physical Review D 70 (2004) 092007
  vector slope and curvature to be
  $(20.64 \pm 1.75) \times 10^{-3}$, $(3.20 \pm 0.69) \times 10^{-3}$ and scalar slope to
  $(13.72 \pm 1.31) \times 10^{-3}$ respectively.

KTeV experiment

- KTeV experiment at Fermilab. 1.9 million K_L electron and 1.5 million K_L muono decays.
- T. Alexopoulos et al., Physical Review D 70 (2004) 092007
  vector slope and curvature to be
  $(20.64 \pm 1.75) \times 10^{-3}$, $(3.20 \pm 0.69) \times 10^{-3}$ and scalar slope to
  $(13.72 \pm 1.31) \times 10^{-3}$ respectively.
- New analysis based on dispersive techniques, E. Abouzaid et al., arXiv;0912.1291 takes into account constraints from lattice QCD, resulting in a fit for the form factor at the Callan-Treiman points.

τ decays from BELLE

- D. Epifanov et al., Physics Letters B 654 (2007) 65 reports measurement of modulus and phase of the $K\pi$ form factors in terms of resonances, based on about 53,000 lepton tagged events.

τ decays from BELLE

- D. Epifanov et al., Physics Letters B 654 (2007) 65 reports measurement of modulus and phase of the $K\pi$ form factors in terms of resonances, based on about 53,000 lepton tagged events.
- Note that the measurement here is in the time-like region on the unitarity cut. Produces an important consistency check.

τ decays from BELLE

- D. Epifanov et al., Physics Letters B 654 (2007) 65 reports measurement of modulus and phase of the $K\pi$ form factors in terms of resonances, based on about 53,000 lepton tagged events.
- Note that the measurement here is in the time-like region on the unitarity cut. Produces an important consistency check.
- Mushkelishvili-Omnès study of πK, πK^*, $K\rho$ and use of high statistics LASS experiment phase shifts used to produce the πK vector form factor and compared with BELLE (B. Moussallam, European Physical Journal C 53 (2008) 401)

τ decays from BELLE

- D. Epifanov et al., Physics Letters B 654 (2007) 65 reports measurement of modulus and phase of the $K\pi$ form factors in terms of resonances, based on about 53,000 lepton tagged events.
- Note that the measurement here is in the time-like region on the unitarity cut. Produces an important consistency check.
- Mushkelishvili-Omnès study of πK, πK^*, $K\rho$ and use of high statistics LASS experiment phase shifts used to produce the πK vector form factor and compared with BELLE (B. Moussallam, European Physical Journal C 53 (2008) 401)
- Series of studies based on these data: M. Jamin et al. Physics Letters B 664 (2008) 78; B 640 (2006) 176

  D. R. Boito et al., European Physical Journal C 59 (2009) 821.

Theoretical approaches

- Our work is motivated by the need to exploit in a complete and optimal way the available information.

Theoretical approaches

- Our work is motivated by the need to exploit in a complete and optimal way the available information.
- We use analyticity, dispersion relations and theoretical inputs.

Theoretical approaches

- Our work is motivated by the need to exploit in a complete and optimal way the available information.
- We use analyticity, dispersion relations and theoretical inputs.
- We use experimental scattering phase shifts determined using Roy-Steiner equations via Watson theorem (the phase of the form factor is the scattering phase shift in the elastic region).

Theoretical approaches

- Our work is motivated by the need to exploit in a complete and optimal way the available information.
- We use analyticity, dispersion relations and theoretical inputs.
- We use experimental scattering phase shifts determined using Roy-Steiner equations via Watson theorem (the phase of the form factor is the scattering phase shift in the elastic region).
- Uses experimental information in such a way as to optimize all available inputs, and the modulus information only to evaluate an integral.

Theoretical approaches

- Our work is motivated by the need to exploit in a complete and optimal way the available information.
- We use analyticity, dispersion relations and theoretical inputs.
- We use experimental scattering phase shifts determined using Roy-Steiner equations via Watson theorem (the phase of the form factor is the scattering phase shift in the elastic region).
- Uses experimental information in such a way as to optimize all available inputs, and the modulus information only to evaluate an integral.
- For a guide, we look at the scalar form factor analysis of M. Jamin, J. A. Oller and A. Pich, Nuclear Physics B622 (2002) 279; Physical Review D 74 (2006) 074009.

Theoretical approaches

- Our work is motivated by the need to exploit in a complete and optimal way the available information.
- We use analyticity, dispersion relations and theoretical inputs.
- We use experimental scattering phase shifts determined using Roy-Steiner equations via Watson theorem (the phase of the form factor is the scattering phase shift in the elastic region).
- Uses experimental information in such a way as to optimize all available inputs, and the modulus information only to evaluate an integral.
- For a guide, we look at the scalar form factor analysis of M. Jamin, J. A. Oller and A. Pich, Nuclear Physics B622 (2002) 279; Physical Review D 74 (2006) 074009.
- Our phase and modulus data come from Moussallam, group of Jamin et al., and from BELLE.

QCD correlator $\chi_0(Q^2)$ - I

- Consider the QCD correlator

$$\chi_0(Q^2) \equiv \frac{\partial}{\partial q^2}\left[q^2\Pi_0\right] = \frac{1}{\pi}\int_{t_+}^{\infty} dt\, \frac{t\mathrm{Im}\Pi_0(t)}{(t+Q^2)^2}\,,$$

$$\mathrm{Im}\Pi_0(t) \geq \frac{3}{2}\,\frac{t_+t_-}{16\pi}\,\frac{[(t-t_+)(t-t_-)]^{1/2}}{t^3}\,|f_0(t)|^2\,,$$

with $t_\pm = (M_K \pm M_\pi)^2$.

QCD correlator $\chi_0(Q^2)$ - I

- Consider the QCD correlator

$$\chi_0(Q^2) \equiv \frac{\partial}{\partial q^2}\left[q^2\Pi_0\right] = \frac{1}{\pi}\int_{t_+}^{\infty} dt\, \frac{t\,\mathrm{Im}\Pi_0(t)}{(t+Q^2)^2}\,,$$

$$\mathrm{Im}\Pi_0(t) \geq \frac{3}{2}\,\frac{t_+t_-}{16\pi}\,\frac{[(t-t_+)(t-t_-)]^{1/2}}{t^3}\,|f_0(t)|^2\,,$$

with $t_\pm = (M_K \pm M_\pi)^2$.

- Positive definite and can be bounded.

QCD correlator $\chi_0(Q^2)$ - I

- Consider the QCD correlator

$$\chi_0(Q^2) \equiv \frac{\partial}{\partial q^2}\left[q^2\Pi_0\right] = \frac{1}{\pi}\int_{t_+}^{\infty} dt\, \frac{t\,\mathrm{Im}\Pi_0(t)}{(t+Q^2)^2}\,,$$

$$\mathrm{Im}\Pi_0(t) \geq \frac{3}{2}\,\frac{t_+ t_-}{16\pi}\,\frac{[(t-t_+)(t-t_-)]^{1/2}}{t^3}\,|f_0(t)|^2\,,$$

with $t_\pm = (M_K \pm M_\pi)^2$.

- Positive definite and can be bounded.
- Bounds can be obtained using analyticity to transform the problem, and to input values of the form factor and its derivatives at $t=0$ and/or knowledge at various points in the analyticity region (method of unitarity bounds).

QCD correlator $\chi_0(Q^2)$ - II

- On the other hand, in pQCD when $Q \gg \Lambda_{\rm QCD}$, m_q, α_S $\overline{MS}$ scheme.

$$\chi_0(Q^2) = \frac{3(m_s - m_u)^2}{8\pi^2 Q^2}\left[1 + 1.80\alpha_s + 4.65\alpha_s^2 + 15.0\alpha_s^3 + 57.4\alpha_s^4 \ldots\right].$$

QCD correlator $\chi_0(Q^2)$ - II

- On the other hand, in pQCD when $Q \gg \Lambda_{\rm QCD}$, m_q, α_S $\overline{MS}$ scheme.

$$\chi_0(Q^2) = \frac{3(m_s - m_u)^2}{8\pi^2 Q^2}\left[1 + 1.80\alpha_s + 4.65\alpha_s^2 + 15.0\alpha_s^3 + 57.4\alpha_s^4 \ldots\right].$$

- For details, Gauhar Abbas et al, arXiv:0912.2831, C. Bourrely and Irinel Caprini, Nuclear Physics B722 (2005) 149.

QCD correlator $\chi_0(Q^2)$ - II

- On the other hand, in pQCD when $Q \gg \Lambda_{\mathrm{QCD}}, m_q, \alpha_S$ $\overline{MS}$ scheme.

$$\chi_0(Q^2) = \frac{3(m_s - m_u)^2}{8\pi^2 Q^2}\left[1 + 1.80\alpha_s + 4.65\alpha_s^2 + 15.0\alpha_s^3 + 57.4\alpha_s^4 \ldots\right].$$

- For details, Gauhar Abbas et al, arXiv:0912.2831, C. Bourrely and Irinel Caprini, Nuclear Physics B722 (2005) 149.
- Reverse problem: to constrain λ_0', λ_0'' and $f_0(\Delta_{K\pi})$ and $f_0(\overline{\Delta}_{K\pi})$.

Transforming via Conformal map

$$\frac{z-1}{z+1} = i\sqrt{\frac{t}{t_+} - 1}$$

Transforming via Conformal map

$$\frac{z-1}{z+1} = i\sqrt{\frac{t}{t_+} - 1}$$

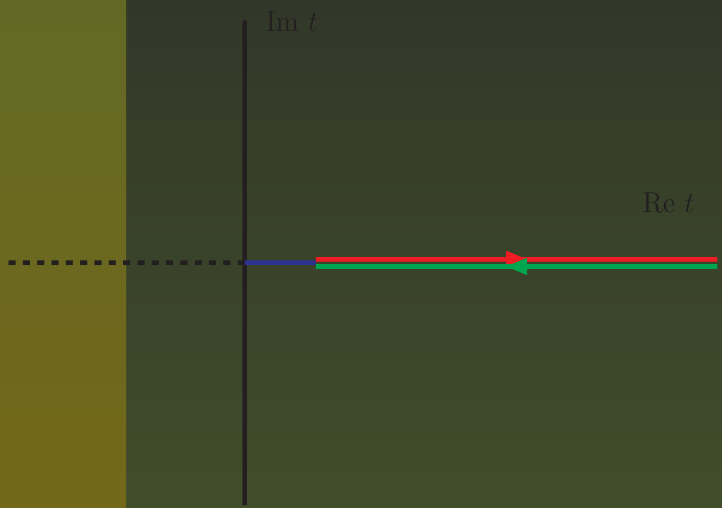

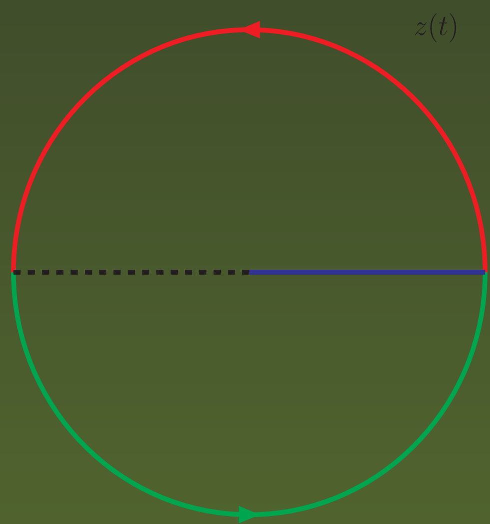

The problem transformed

- We can now use the conformal map to transform this to an integral that reads

$$\frac{1}{2\pi}\int_0^{2\pi} |h(\exp(i\theta))|^2 \leq I_{\rm pQCD}$$

and needs to be bounded.

The problem transformed

- We can now use the conformal map to transform this to an integral that reads

$$\frac{1}{2\pi}\int_0^{2\pi} |h(\exp(i\theta))|^2 \leq I_{\mathrm{pQCD}}$$

  and needs to be bounded.

- This requires the knowledge of the **outer function** associated with the function multiplying $|f_0(t)|^2$ and the Jacobian of the transformation.

The problem transformed

- We can now use the conformal map to transform this to an integral that reads

$$\frac{1}{2\pi}\int_0^{2\pi} |h(\exp(i\theta))|^2 \le I_{\rm pQCD}$$

  and needs to be bounded.

- This requires the knowledge of the **outer function** associated with the function multiplying $|f_0(t)|^2$ and the Jacobian of the transformation.

- For the case at hand:

$$\begin{aligned} w(z) &= \frac{3}{16\sqrt{2\pi}}\,\frac{M_K-M_\pi}{M_K+M_\pi}\sqrt{1-z}\,(1+z)^{3/2} \\ &\quad\times\frac{(1+z(-Q^2))^2}{(1-z\,z(-Q^2))^2}\,\frac{(1-z\,z(t_-))^{1/2}}{(1+z(t_-))^{1/2}}, \\ h(z) &= w(z)f_0(z). \end{aligned}$$

Power series and origin of the bound

- Power series: $h(z) = a_0 + a_1 z + a_2 z^2 + \ldots$ [Fourier series with non-negative powers of $e^{i\theta}$]. Guaranteed for such functions.

Power series and origin of the bound

- Power series: $h(z) = a_0 + a_1 z + a_2 z^2 + \ldots$ [Fourier series with non-negative powers of $e^{i\theta}$]. Guaranteed for such functions.
- Very important to note that the origin in the complex-t plane is mapped to the origin in the complex-z plane. Expansion in powers of z is related to expansion in powers of t, which is why slope and curvature parameters enter here.

Power series and origin of the bound

- Power series: $h(z) = a_0 + a_1 z + a_2 z^2 + \ldots$ [Fourier series with non-negative powers of $e^{i\theta}$]. Guaranteed for such functions.
- Very important to note that the origin in the complex-t plane is mapped to the origin in the complex-z plane. Expansion in powers of z is related to expansion in powers of t, which is why slope and curvature parameters enter here.
- Furthermore and significantly, square integrability implies $I = |a_0|^2 + |a_1|^2 + \ldots$ [Parseval theorem]

Power series and origin of the bound

- Power series: $h(z) = a_0 + a_1 z + a_2 z^2 + \ldots$ [Fourier series with non-negative powers of $e^{i\theta}$]. Guaranteed for such functions.
- Very important to note that the origin in the complex-t plane is mapped to the origin in the complex-z plane. Expansion in powers of z is related to expansion in powers of t, which is why slope and curvature parameters enter here.
- Furthermore and significantly, square integrability implies $I = |a_0|^2 + |a_1|^2 + \ldots$ [Parseval theorem]
- Outer function is known and can be expanded in a series in z.

Power series and origin of the bound

- Power series: $h(z) = a_0 + a_1 z + a_2 z^2 + \ldots$ [Fourier series with non-negative powers of $e^{i\theta}$]. Guaranteed for such functions.
- Very important to note that the origin in the complex-t plane is mapped to the origin in the complex-z plane. Expansion in powers of z is related to expansion in powers of t, which is why slope and curvature parameters enter here.
- Furthermore and significantly, square integrability implies $I = |a_0|^2 + |a_1|^2 + \ldots$ [Parseval theorem]
- Outer function is known and can be expanded in a series in z.
- If the first n coefficients of the form factor are known, a bound on the quantity of interest is obtained after a finite number of terms.

Some explicit expressions

- $$a_0 = h(0) = f_+(0)w(0),$$

Some explicit expressions

- $$a_0 = h(0) = f_+(0)w(0),$$

- $$a_1 = h'(0) = f_+(0)(w'(0) + \frac{2}{3}\langle r^2_{\pi \mathrm{K}}\rangle t_+ w(0)),$$

Some explicit expressions

- $$a_0 = h(0) = f_+(0)w(0),$$

- $$a_1 = h'(0) = f_+(0)(w'(0) + \frac{2}{3}\langle r^2_{\pi K}\rangle t_+ w(0)),$$

- $$\begin{aligned} a_2 &= \frac{h''(0)}{2!} = \frac{f_+(0)}{2}\left[w(0)\left(-\frac{8}{3}\langle r^2_{\pi K}\rangle t_+ + 32\,c\,t_+^2\right)\right] \\ &+ \frac{f_+(0)}{2}\left[2w'(0)\left(\frac{2}{3}\langle r^2_{\pi K}\rangle t_\pi\right) + w''(0)\right], \end{aligned}$$

Improving the bounds

- Improvement of the bound arises if $f_0(t)$ is known for some spacelike values of momenta corresponding to $z = x_i,\ i = 1, 2, 3, ...$

Improving the bounds

- Improvement of the bound arises if $f_0(t)$ is known for some spacelike values of momenta corresponding to $z = x_i,\ i = 1, 2, 3, ...$
- Improve the bound by using imposing constraints using Lagrange multipliers.

Improving the bounds

- Improvement of the bound arises if $f_0(t)$ is known for some spacelike values of momenta corresponding to $z = x_i$, $i = 1, 2, 3, ...$
- Improve the bound by using imposing constraints using Lagrange multipliers.
- Can also be improved by imposing phase of the form factor for timelike moment in a continuous region, $a \leq t \leq b$.

Timelike data – Introduction

- Extend the analysis to include timelike data [phase only].
  (Timelike phase and no spacelike constraints done by Caprini)

Timelike data – Introduction

- Extend the analysis to include timelike data [phase only]. (Timelike phase and no spacelike constraints done by Caprini)
- Recall Watson's theorem:

$$\mathrm{Arg}[F(t+i\epsilon)] = \delta_0^{1/2}(t), \; t_\pi < t < t_{in},$$

where $\delta_0^{1/2}(t)$ is the scattering phase shift obtained from experiment.

Timelike data – Introduction

- Extend the analysis to include timelike data [phase only]. (Timelike phase and no spacelike constraints done by Caprini)
- Recall Watson's theorem:

$$\mathrm{Arg}[F(t+i\epsilon)] = \delta_0^{1/2}(t),\; t_\pi < t < t_{in},$$

where $\delta_0^{1/2}(t)$ is the scattering phase shift obtained from experiment.

- Phase constraint introduced via Omnès function

Definitions

$$\overline{\delta}_0^{1/2}(\theta) \equiv \mathrm{Arg}[F(r\exp i\theta)]$$

$$\overline{\delta}_0^{1/2}(\theta) = \begin{cases} \delta_0^{1/2}(\theta),\ 0 \le \theta \le \theta_{in} \\ -\delta_0^{1/2}(\theta),\ 2\pi - \theta_{in} \le \theta \le 0 \end{cases}$$

Definitions

- $$\overline{\delta}_0^{1/2}(\theta) \equiv \mathrm{Arg}[F(r\exp i\theta)]$$
$$\overline{\delta}_0^{1/2}(\theta) = \begin{array}{c} \delta_0^{1/2}(\theta),\ 0 \le \theta \le \theta_{in} \\ -\delta_0^{1/2}(\theta),\ 2\pi - \theta_{in} \le \theta \le 0 \end{array}$$

- $$\mathcal{O}(z) = \exp[\frac{i}{\pi}\int_0^{2\pi} d\theta \frac{\overline{\delta}_0^{1/2}(\theta)}{1 - z\exp(i\theta)}]$$
$$W(\zeta) = \omega_\pi(\zeta)\mathcal{O}(\zeta),\ W(\theta) = |W(\theta)|\exp(i\Phi(\theta))$$

This function is used to implement the constraint stemming from knowledge of phase of the form factor.

Generalized Lagrange multiplier

Introduce now the Lagrangian (here $J = h(z)$):

$$\mathcal{L} = \frac{1}{2}\sum_n a_n^2$$

$$+ \frac{1}{\pi}\sum_n a_n \lim_{r\to 1}\int_\Gamma \lambda(\theta)|W(\theta)|[\mathrm{Im}[W(\theta)]^{-1} r^n \exp(i\theta)]d\theta$$

$$+ \alpha(J - \textstyle\sum_n a_n z^n)$$

Map showing region of integration

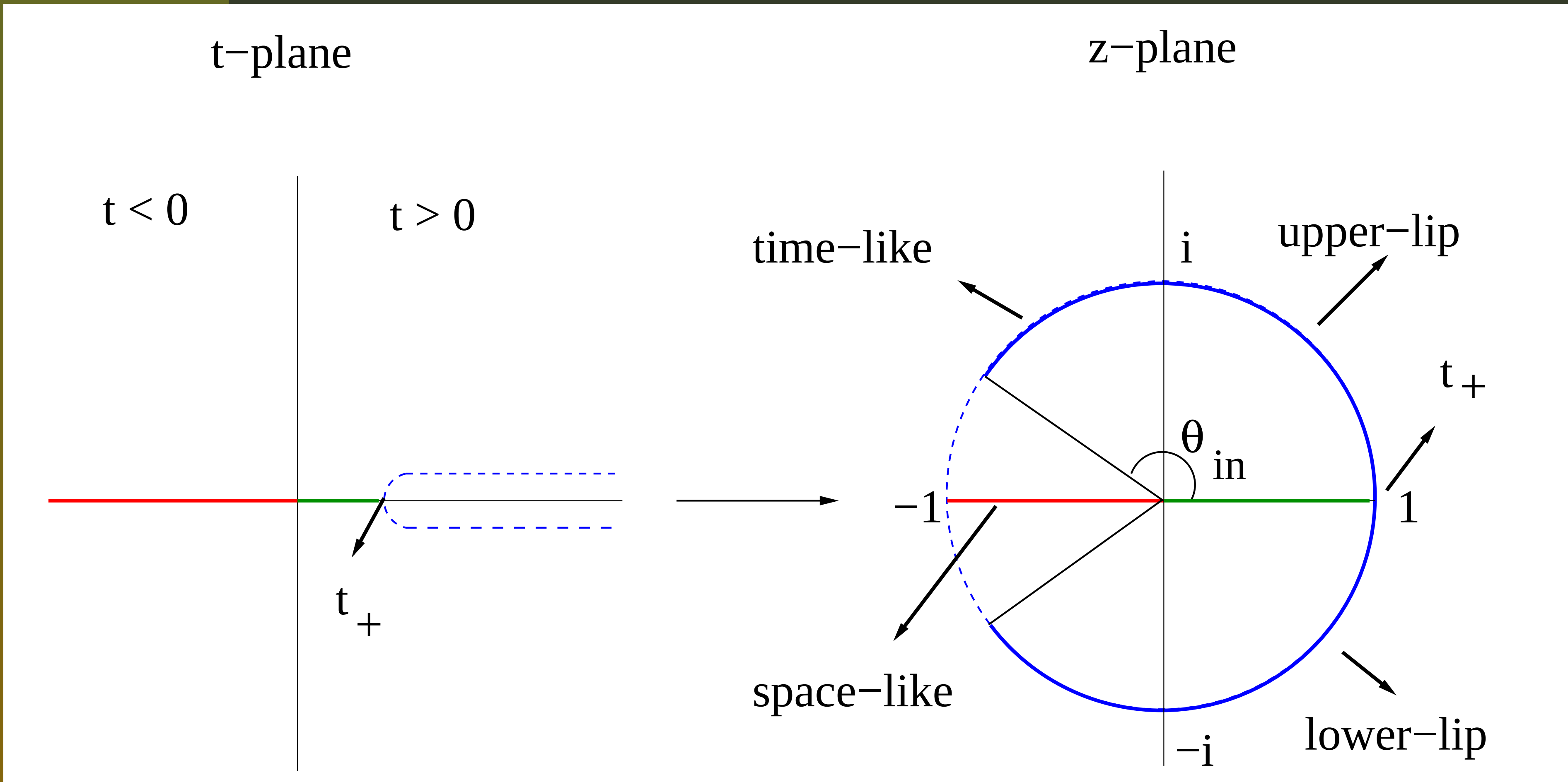

Equations for Lagrange multipliers I

- Working out the minimization conditions and simplification, the result may be expressed elegantly in terms of two coupled equations for $\lambda(\theta)$ and α.

Equations for Lagrange multipliers I

- Working out the minimization conditions and simplification, the result may be expressed elegantly in terms of two coupled equations for $\lambda(\theta)$ and α.
- These are the generalized Lagrange multiplier associated with the phase, and Lagrange multiplier associated with the spacelike constraint respectively, when the first N coefficients are held fixed.

Equations for Lagrange multipliers II

$$\lambda(\theta) = \sum_{n=0}^{N} a_n \left[\sin(n\theta - \Phi(\theta)) - \frac{1-z^2}{z^{N+1}}\beta(\theta)z^n\right] +$$

$$\frac{1}{\pi}\int_\Gamma d\theta'\lambda(\theta')\frac{1}{2}\frac{\sin[(N+1/2)(\theta-\theta') - \Phi(\theta) + \Phi(\theta')]}{\sin[\frac{\theta-\theta'}{2}]} +$$

$$\frac{1}{\pi}\int_\Gamma d\theta'\lambda(\theta')(1-z^2)\beta(\theta)\beta(\theta')d\theta' + J\frac{1-z^2}{z^{N+1}}\beta(\theta),$$

$$\beta(\theta) = \frac{\sin[(N+1)\theta - \Phi(\theta)] - z\sin[N\theta - \Phi(\theta)]}{1+z^2-2z\cos(\theta)}$$

Equations for Lagrange multipliers II

- $$\lambda(\theta) = \sum_{n=0}^{N} a_n \left[\sin(n\theta - \Phi(\theta)) - \frac{1-z^2}{z^{N+1}}\beta(\theta) z^n\right] +$$
$$\frac{1}{\pi}\int_\Gamma d\theta' \lambda(\theta') \frac{1}{2} \frac{\sin[(N+1/2)(\theta-\theta') - \Phi(\theta) + \Phi(\theta')]}{\sin[\frac{\theta-\theta'}{2}]} +$$
$$\frac{1}{\pi}\int_\Gamma d\theta' \lambda(\theta')(1-z^2)\beta(\theta)\beta(\theta') d\theta' + J\frac{1-z^2}{z^{N+1}}\beta(\theta),$$
$$\beta(\theta) = \frac{\sin[(N+1)\theta - \Phi(\theta)] - z\sin[N\theta - \Phi(\theta)]}{1+z^2-2z\cos(\theta)}$$

- $$\alpha = \frac{1-z^2}{(z^2)^{N+1}}\left[J - \sum_{n=0}^{N} + \frac{z^{N+1}}{\pi}\int_\Gamma d\theta' \lambda(\theta')\beta(\theta')\right]$$

Discussion on equations and the bound

- The expression for the bound reads:

$$\sum_{n=0}^{N} a_n^2 + \frac{1}{\pi}\sum_{n=0}^{N}\int_\Gamma d\theta\lambda(\theta)\sin[n\theta-\Phi(\theta)] + \alpha(J - \sum_{n=0}^{N} a_n z^n)$$

Discussion on equations and the bound

- The expression for the bound reads:

$$\sum_{n=0}^{N} a_n^2 + \frac{1}{\pi}\sum_{n=0}^{N}\int_{\Gamma} d\theta\lambda(\theta)\sin[n\theta - \Phi(\theta)] + \alpha(J - \sum_{n=0}^{N} a_n z^n)$$

- The striking feature of this result is as though the contribution of the timelike result is independent of the spacelike result and *vice versa*. However, each has the knowledge of the other as outlined earlier.

Improved bound with several space-like constraints

- Can be extended to arbitrary number of such constraints, and mixed constraints (Meiman problem). The problem solved in generality by A. Raina and V. Singh, Journal of Physics G3 (1977) 315.

Improved bound with several space-like constraints

- Can be extended to arbitrary number of such constraints, and mixed constraints (Meiman problem). The problem solved in generality by A. Raina and V. Singh, Journal of Physics G3 (1977) 315.
- The case of two spacelike constraints is one where we solve:

$$\begin{vmatrix} I & a_0 & a_1 & a_2 & J_1 & J_2 \\ a_0 & 1 & 0 & 0 & 1 & 1 \\ a_1 & 0 & 1 & 0 & x_1 & x_2 \\ a_2 & 0 & 0 & 1 & x_1^2 & x_2^2 \\ J_1 & 1 & x_1 & x_1^2 & (1-x_1^2)^{-1} & (1-x_1 x_2)^{-1} \\ J_2 & 1 & x_2 & x_2^2 & (1-x_1^2)^{-1} & (1-x_2^2)^{-1} \end{vmatrix} = 0$$

to obtain the bound, if a_i and J_i are known. Here I and J_i are known, and hence we can bound the a_i!

Illustration of two constraints

- Results from imposing constraints from CT1 and CT2

Illustration of two constraints

- Results from imposing constraints from CT1 and CT2
- Zoom into the region isolated by the constraints and sensitivity to value at CT2

Illustration of two constraints

- Results from imposing constraints from CT1 and CT2
- Zoom into the region isolated by the constraints and sensitivity to value at CT2
- Gauhar Abbas and BA, European Physical Journal A 41 (2009) 7.

Cartoon with 0, 1 and 2 constraints

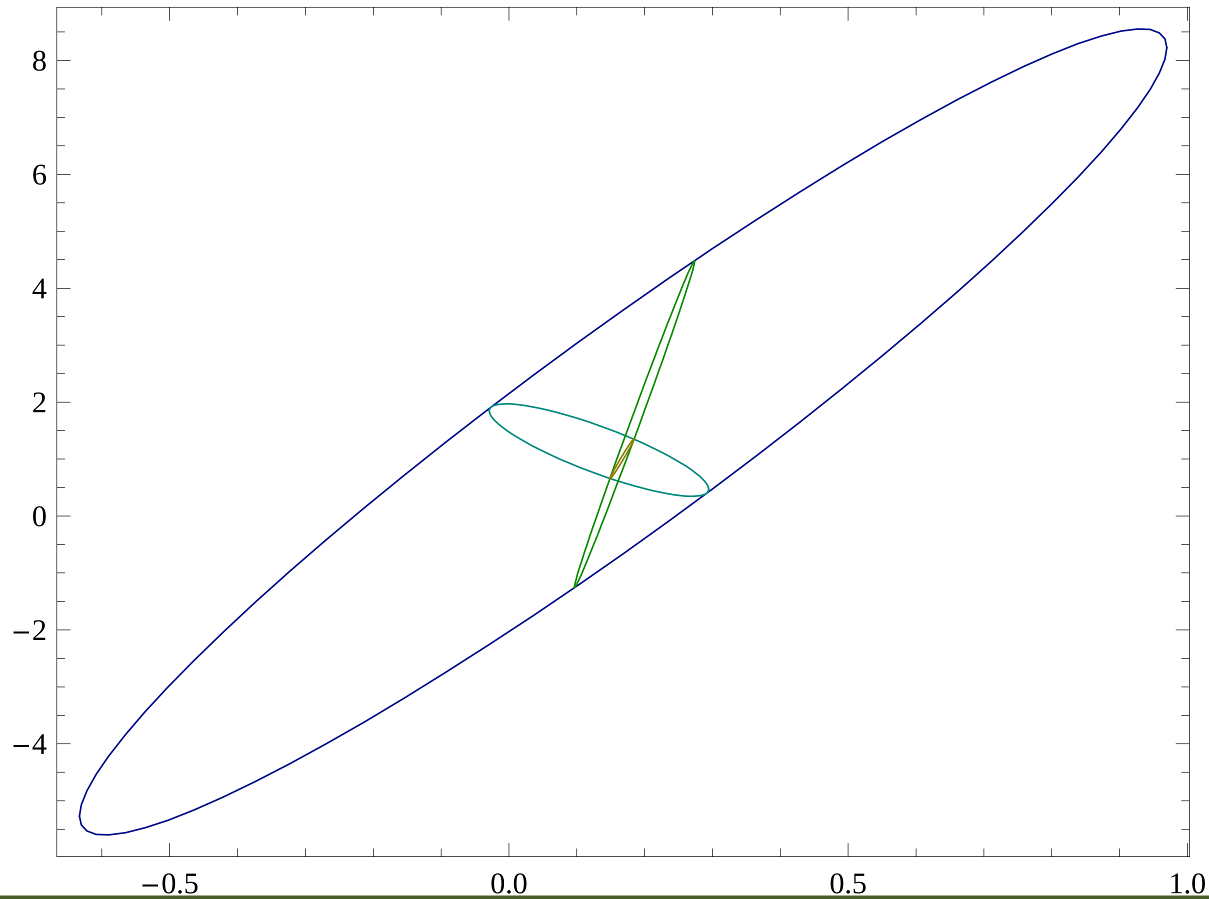

Results with 1 and 2 constraints

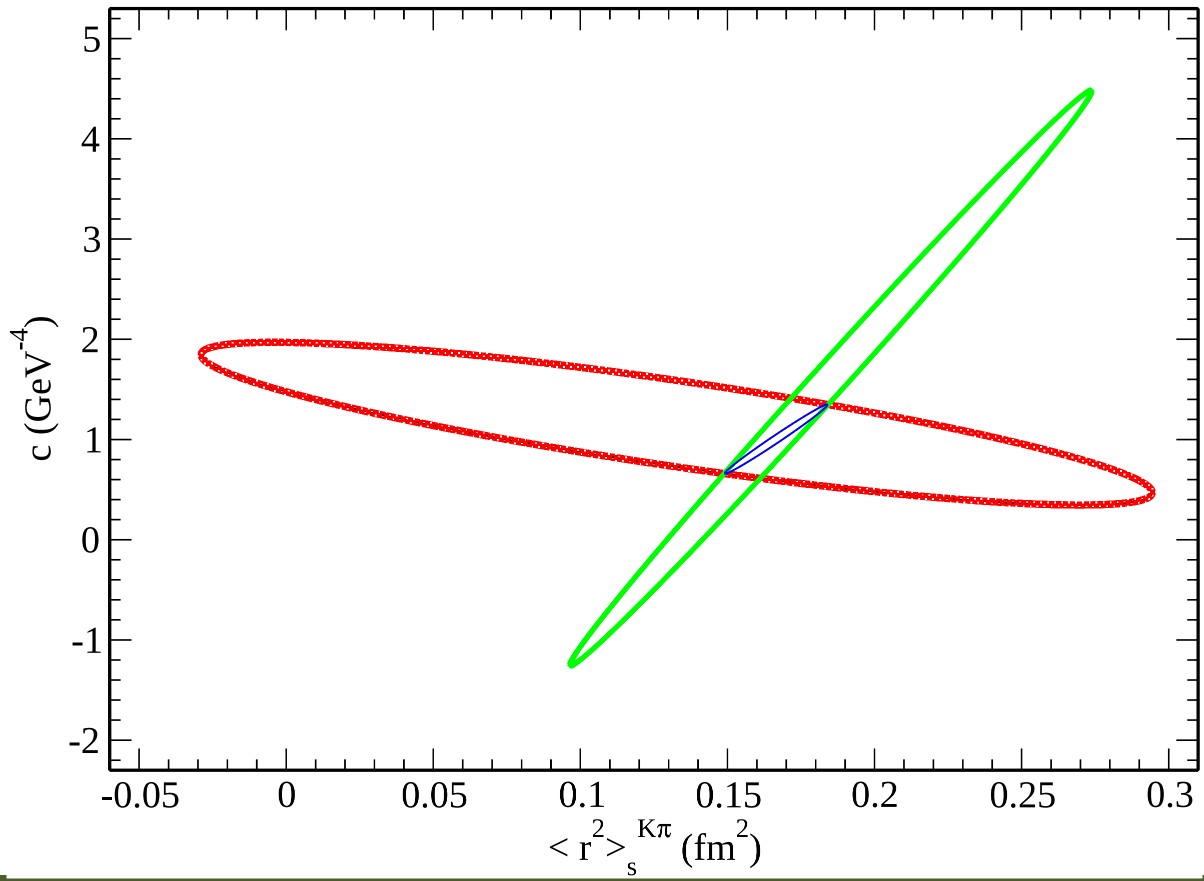

Results with variation at CT_2 by 3%

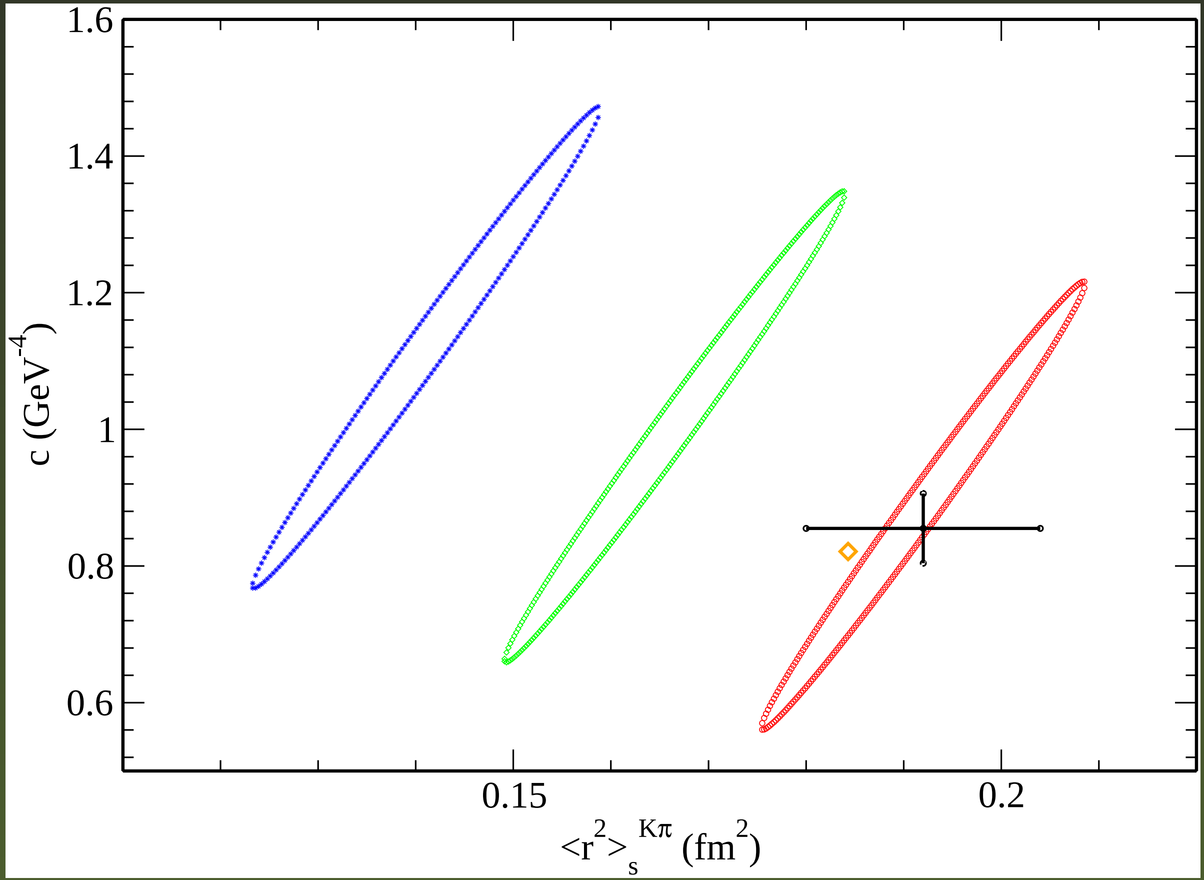

Inclusion of phase and modulus

- In the elastic region, the phase of the form factor is the scattering phase (Watson's theorem). Can be included using Lagrange multipliers to obtain improved optimal constraints (already discussed).

Inclusion of phase and modulus

- In the elastic region, the phase of the form factor is the scattering phase (Watson's theorem). Can be included using Lagrange multipliers to obtain improved optimal constraints (already discussed).
- Availability of phase of the form factor and modulus can be used to find even more stringent constraints by adapting the formalism given earlier.

Inclusion of phase and modulus

- In the elastic region, the phase of the form factor is the scattering phase (Watson's theorem). Can be included using Lagrange multipliers to obtain improved optimal constraints (already discussed).
- Availability of phase of the form factor and modulus can be used to find even more stringent constraints by adapting the formalism given earlier.
- Adaptation of method first proposed by Caprini in 1999 in the context of the pion electromagnetic form factor (I. Caprini, European Physical Journal C 13 (2000) 471).

Inclusion of phase and modulus

- In the elastic region, the phase of the form factor is the scattering phase (Watson's theorem). Can be included using Lagrange multipliers to obtain improved optimal constraints (already discussed).
- Availability of phase of the form factor and modulus can be used to find even more stringent constraints by adapting the formalism given earlier.
- Adaptation of method first proposed by Caprini in 1999 in the context of the pion electromagnetic form factor (I. Caprini, European Physical Journal C 13 (2000) 471).
- The present work is the only other known application of this powerful technique which is described in the following.

Omnès function

- Consider the definition

$$\mathcal{O}(t) = \exp\left(\frac{t}{\pi}\int_{t_+}^{\infty} dt \frac{\delta(t')}{t'(t'-t)}\right),$$

where $\delta(t)$ is the $I = 1/2$ elastic S-wave $K\pi$ scattering phase, in the elastic region and arbitrary Lipschitz continuous above t_{in} (viz., the phase and its first derivative are continuous).

Omnès function

- Consider the definition

$$\mathcal{O}(t) = \exp\left(\frac{t}{\pi}\int_{t_+}^{\infty} dt \frac{\delta(t')}{t'(t'-t)}\right),$$

where $\delta(t)$ is the $I = 1/2$ elastic S-wave $K\pi$ scattering phase, in the elastic region and arbitrary Lipschitz continuous above t_{in} (viz., the phase and its first derivative are continuous).

- Since the Omnès function $\mathcal{O}(t)$ fully accounts for the second Riemann sheet of the form factor, the function $h(t)$, defined by

$$f_0(t) = h(t)\,\mathcal{O}(t),$$

is real analytic in the t-plane with a cut only for $t \geq t_{\rm in}$.

Omnès function

- Consider the definition

$$\mathcal{O}(t) = \exp\left(\frac{t}{\pi}\int_{t_+}^{\infty} dt \frac{\delta(t')}{t'(t'-t)}\right),$$

where $\delta(t)$ is the $I = 1/2$ elastic S-wave $K\pi$ scattering phase, in the elastic region and arbitrary Lipschitz continuous above t_{in} (viz., the phase and its first derivative are continuous).

- Since the Omnès function $\mathcal{O}(t)$ fully accounts for the second Riemann sheet of the form factor, the function $h(t)$, defined by

$$f_0(t) = h(t)\,\mathcal{O}(t),$$

is real analytic in the t-plane with a cut only for $t \geq t_{\rm in}$.

- Extremely clever trick which makes the method very useful

New conformal map

- The new conformal variable is now:

$$z(t) = \frac{\sqrt{t_{\rm in}} - \sqrt{t_{\rm in} - t}}{\sqrt{t_{\rm in}} + \sqrt{t_{\rm in} - t}},$$

which maps the t-plane cut for $t > t_{\rm in}$ onto the unit disk $|z| < 1$, and

$$h(z) = f_0(t(z))\, w(z)\, \omega(z)\, [\mathcal{O}(t(z))]^{-1},$$

New conformal map

- The new conformal variable is now:

$$z(t) = \frac{\sqrt{t_{\rm in}} - \sqrt{t_{\rm in} - t}}{\sqrt{t_{\rm in}} + \sqrt{t_{\rm in} - t}},$$

which maps the t-plane cut for $t > t_{\rm in}$ onto the unit disk $|z| < 1$, and

$$h(z) = f_0(t(z))\, w(z)\, \omega(z)\, [\mathcal{O}(t(z))]^{-1},$$

- Note that the Omnès function makes an appearance through its outer function, and once as an inverse.

New Outer functions

- The new outer function is

$$w(z) \quad = \quad \frac{3(M_K^2 - M_\pi^2)}{16\sqrt{2\pi}t_{\rm in}} \frac{\sqrt{1-z}\,(1+z)^{3/2}(1+z(-Q^2))^2}{(1-z\,z(-Q^2))^2}$$
$$\times \frac{(1-z\,z(t_+))^{1/2}\,(1-z\,z(t_-))^{1/2}}{(1+z(t_+))^{1/2}\,(1+z(t_-))^{1/2}},$$

New Outer functions

- The new outer function is

$$w(z) \quad = \quad \frac{3(M_K^2 - M_\pi^2)}{16\sqrt{2\pi}t_{\rm in}} \frac{\sqrt{1-z}\,(1+z)^{3/2}(1+z(-Q^2))^2}{(1-z\,z(-Q^2))^2}$$
$$\times \frac{(1-z\,z(t_+))^{1/2}\,(1-z\,z(t_-))^{1/2}}{(1+z(t_+))^{1/2}\,(1+z(t_-))^{1/2}},$$

- An additional outer function now enters which is given by

$$\omega(z) = \exp\left(\frac{\sqrt{t_{\rm in}-t}}{\pi}\int_{t_{\rm in}}^{\infty} dt'\,\frac{\ln|\mathcal{O}(t')|}{\sqrt{t'-t_{\rm in}}(t'-t)}\right).$$

New Outer functions

- The new outer function is

$$w(z) \quad = \quad \frac{3(M_K^2 - M_\pi^2)}{16\sqrt{2\pi} t_{\rm in}} \frac{\sqrt{1-z}\,(1+z)^{3/2}(1+z(-Q^2))^2}{(1-z\,z(-Q^2))^2}$$
$$\times \frac{(1-z\,z(t_+))^{1/2}\,(1-z\,z(t_-))^{1/2}}{(1+z(t_+))^{1/2}\,(1+z(t_-))^{1/2}},$$

- An additional outer function now enters which is given by

$$\omega(z) = \exp\left(\frac{\sqrt{t_{\rm in}-t}}{\pi}\int_{t_{\rm in}}^{\infty} dt'\,\frac{\ln|\mathcal{O}(t')|}{\sqrt{t'-t_{\rm in}}(t'-t)}\right).$$

- The input for the bound is now given by

$$I = \chi_0(Q^2) - \frac{3}{2}\frac{t_+ t_-}{16\pi^2}\int_{t_+}^{t_{\rm in}} dt\,\frac{[(t-t_+)(t-t_-)]^{1/2}|f_0(t)|^2}{t^2(t+Q^2)^2}.$$

The information of the modulus used in an average manner.

Results of analysis with phase and modulus information

- Dependence on parametrization

Results of analysis with phase and modulus information

- Dependence on parametrization
- Dependence on constraints and on t_{in}

Results of analysis with phase and modulus information

- Dependence on parametrization
- Dependence on constraints and on t_{in}
- Gauhar Abbas, BA, I. Caprini, I. Sentitemsu Imsong and S. Ramanan, European Physical Journal A 44 (2010) 175.

With and without phase and modulus, (2 parametrizations).

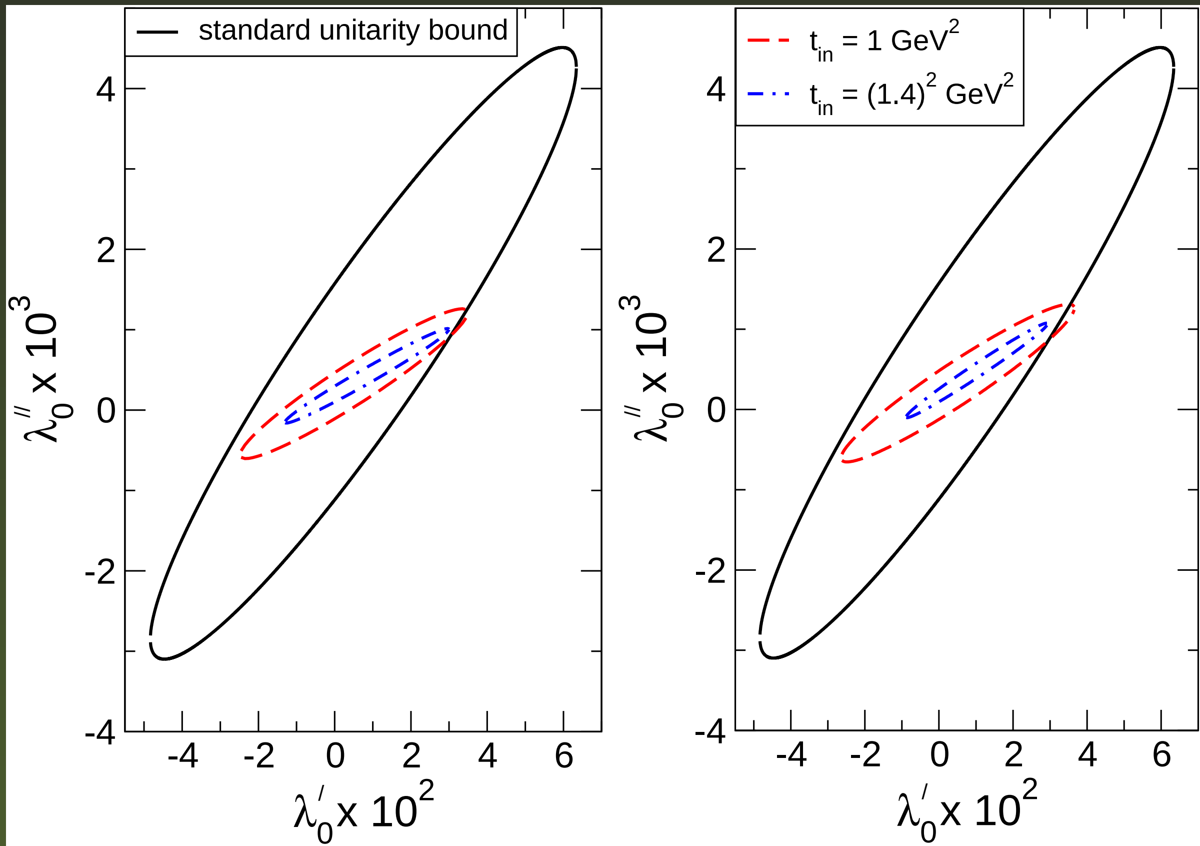

CT_1, and CT_1 and CT_2 constraints

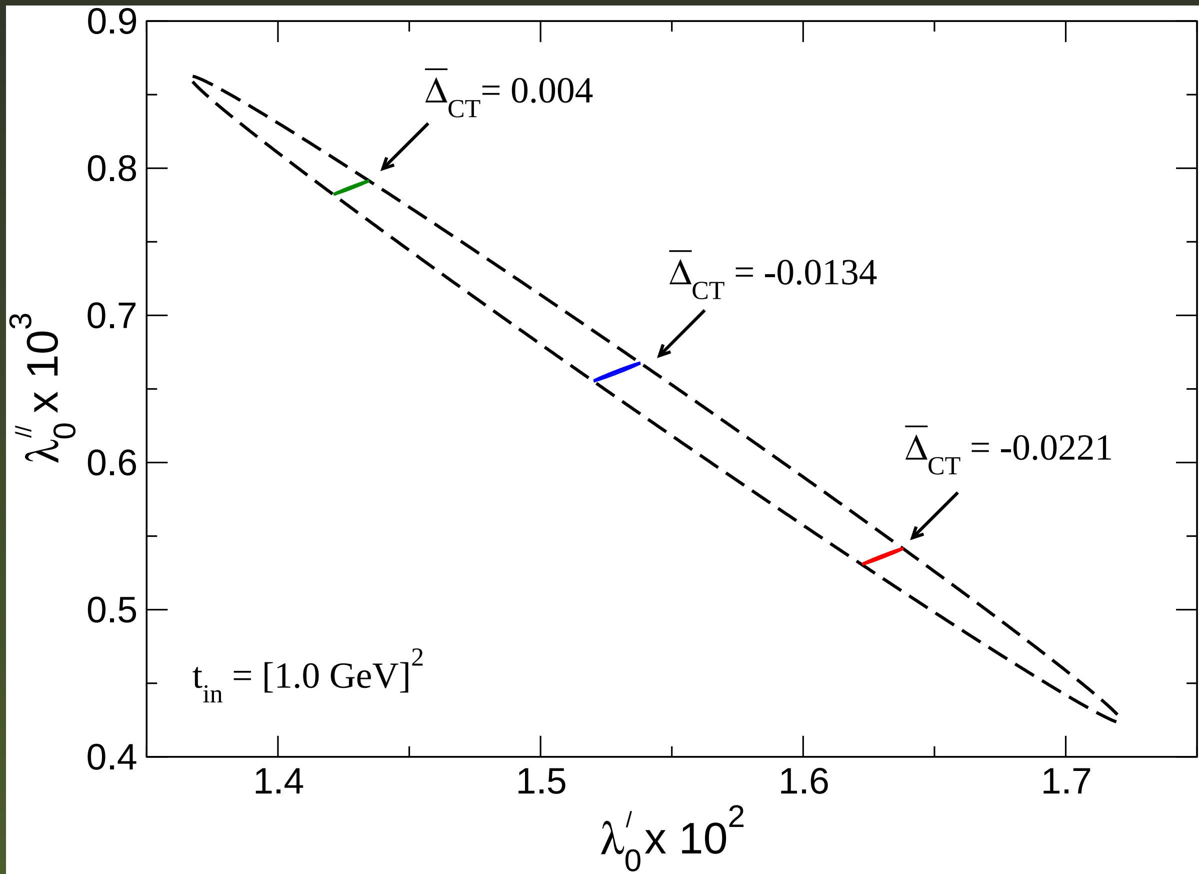

Allowed regions for 2 values of t_{in}

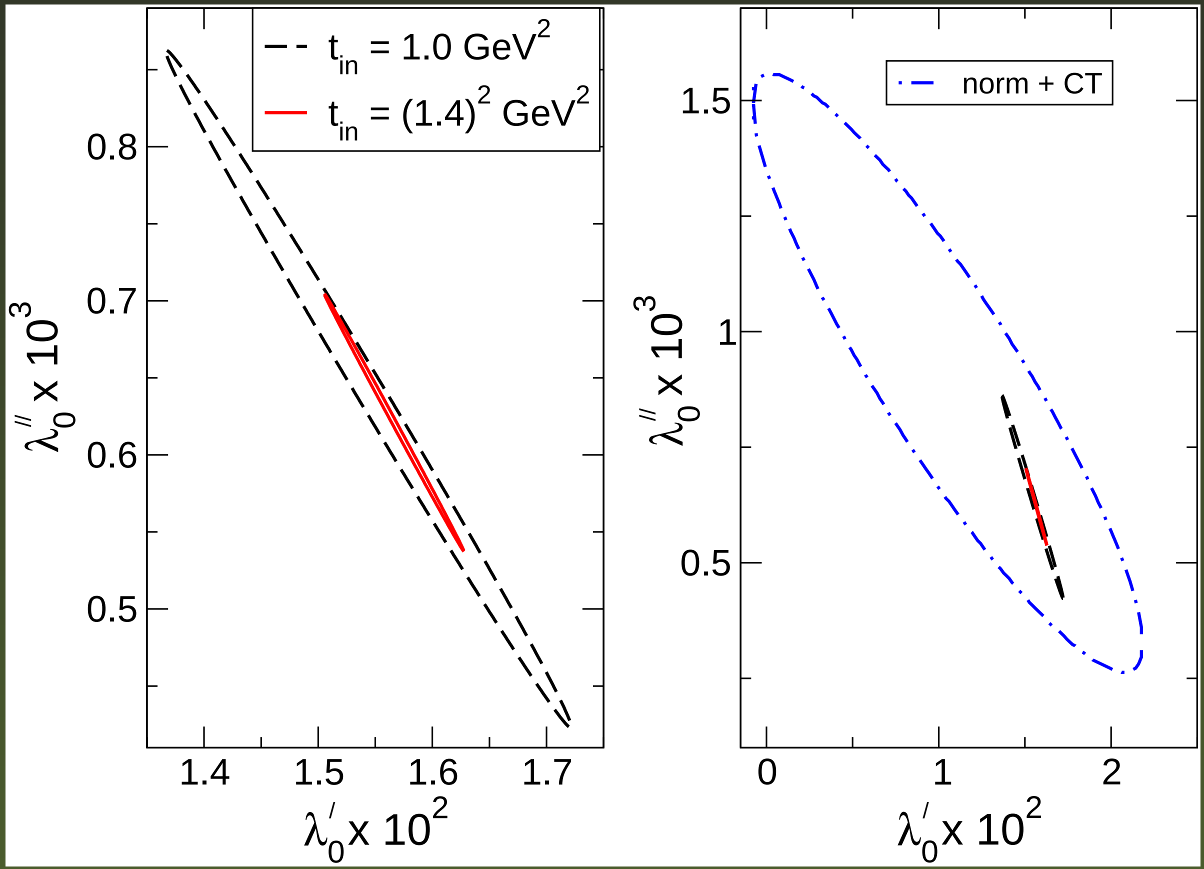

Comparison of Allowed regions with phase (and modulus) with $t_{in} = 1^2$ GeV^2

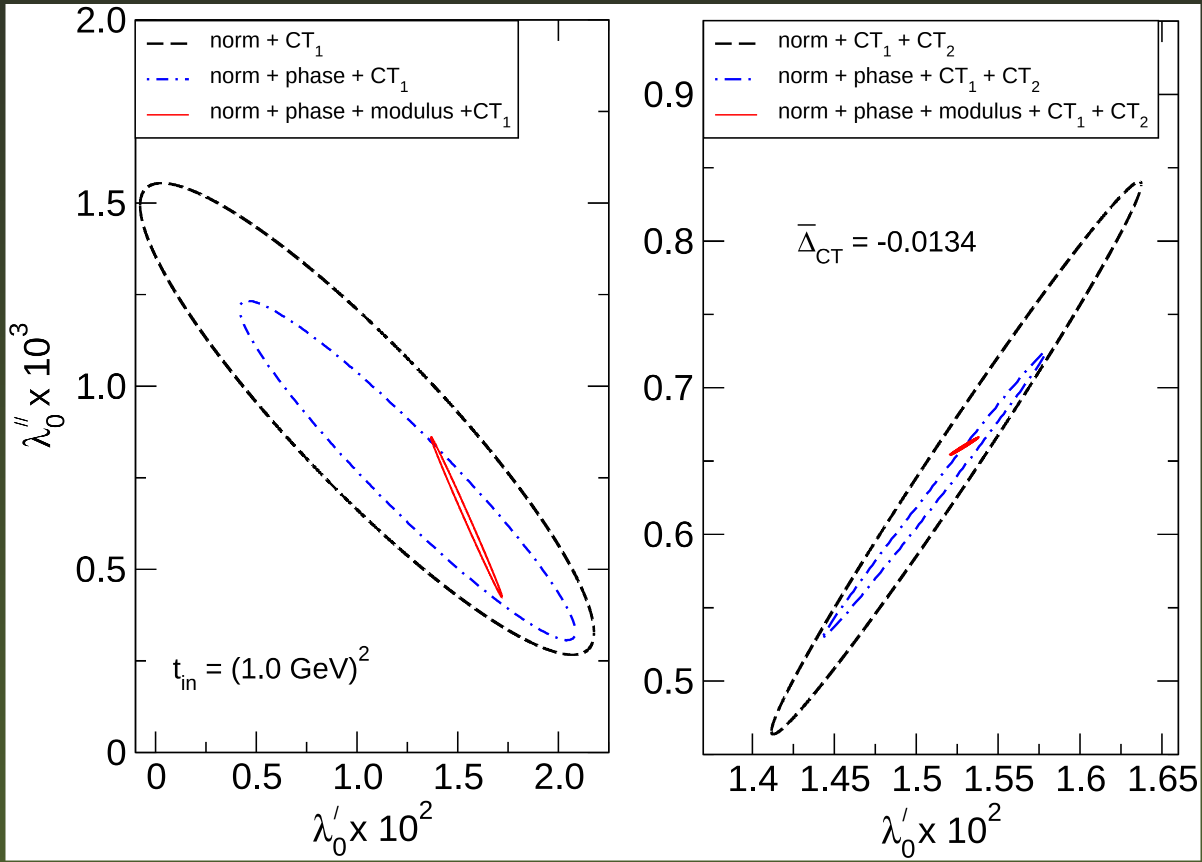

Comparison of results with and without modulus information

- Dependence on t_{in}.

Comparison of results with and without modulus information

- Dependence on t_{in}.
- Dependence on constraints.

Comparison of Allowed regions with phase (and modulus) with $t_{in} = 1.2^2$ GeV^2

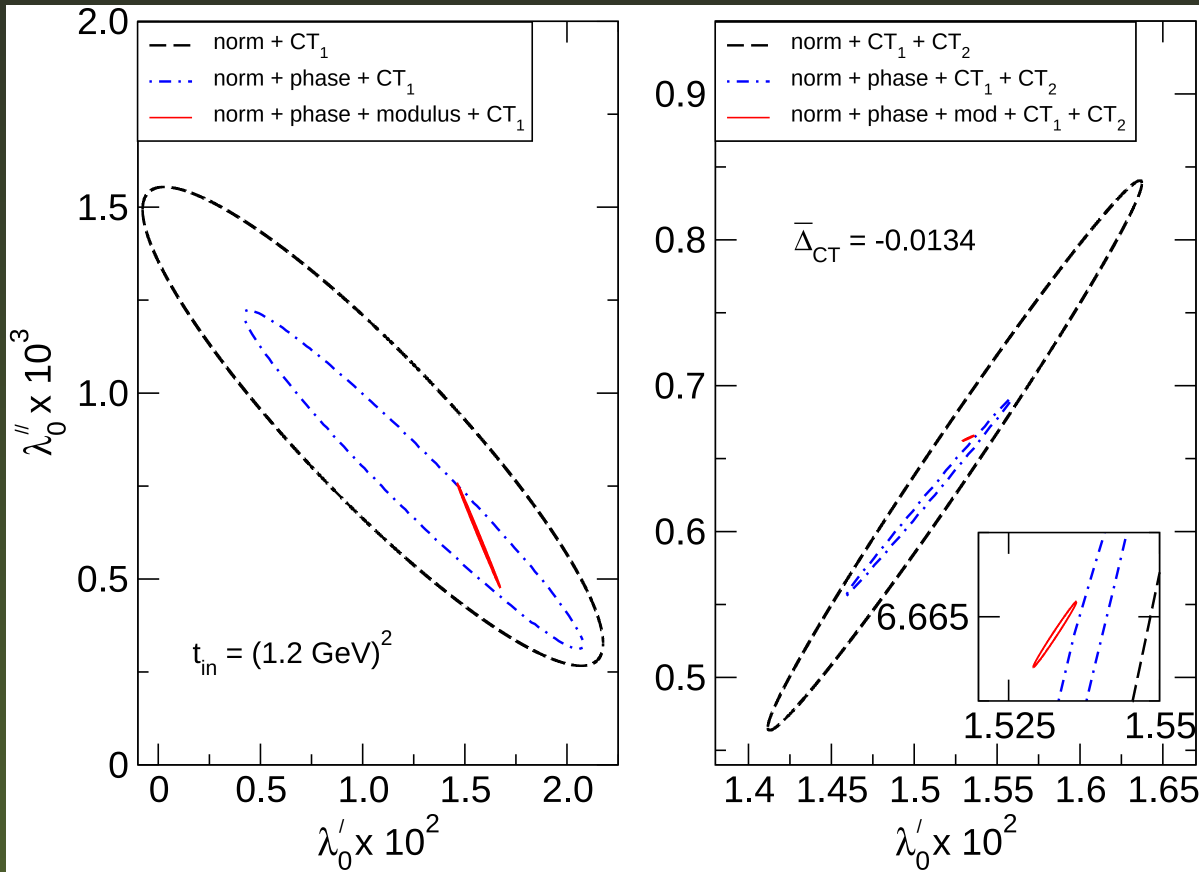

Comparison of Allowed regions with phase (and modulus) with $t_{in} = 1.4^2$ GeV^2

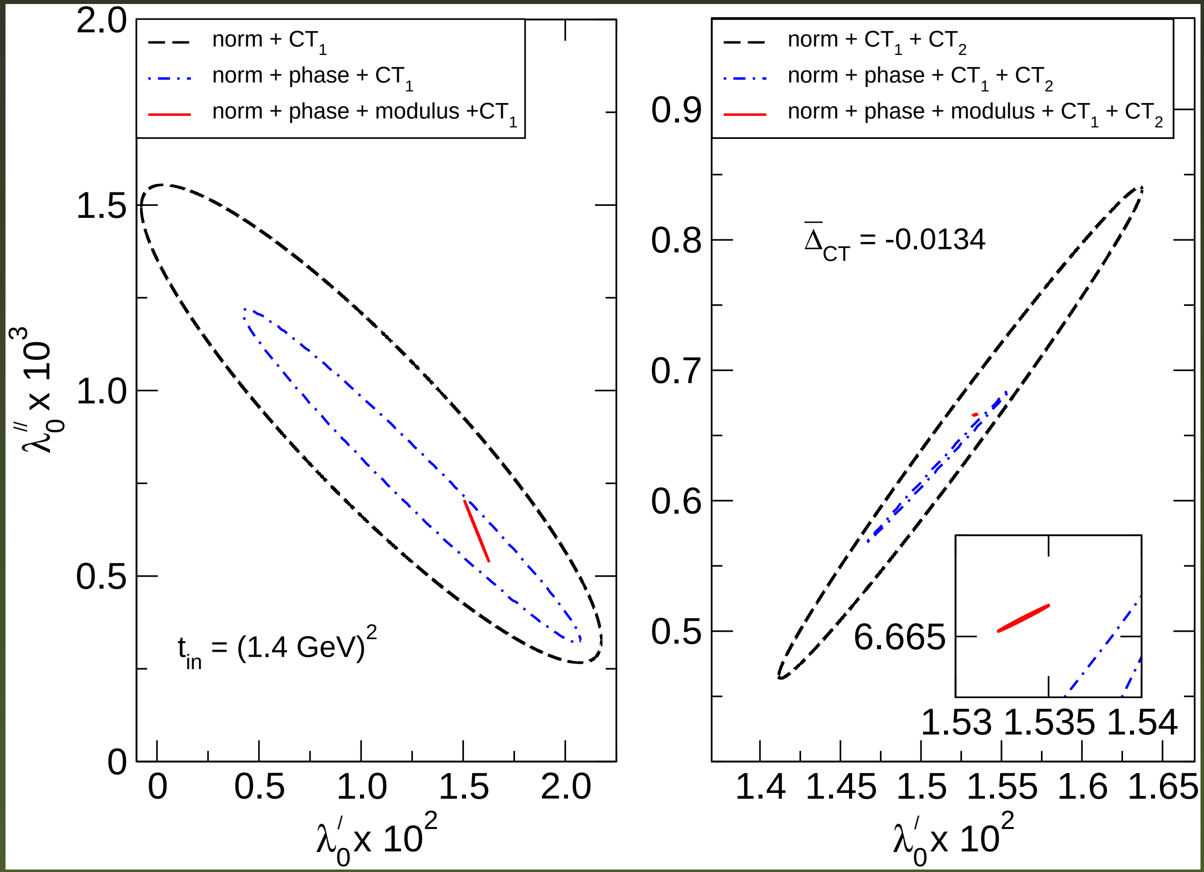

Explicit demonstration of modulus vs. no modulus

- Results with just CT1

Explicit demonstration of modulus vs. no modulus

- Results with just CT1
- Overconstraining due to constraints from CT1 and CT2

Explicit demonstration of modulus vs. no modulus

- Results with just CT1
- Overconstraining due to constraints from CT1 and CT2
- Gauhar Abbas, BA, I. Caprini, I. Sentitemsu Imsong and S. Ramanan, arXiv: 1004.4257

Comparison of Allowed regions with phase (and modulus) with different values of t_{in} and CT_1

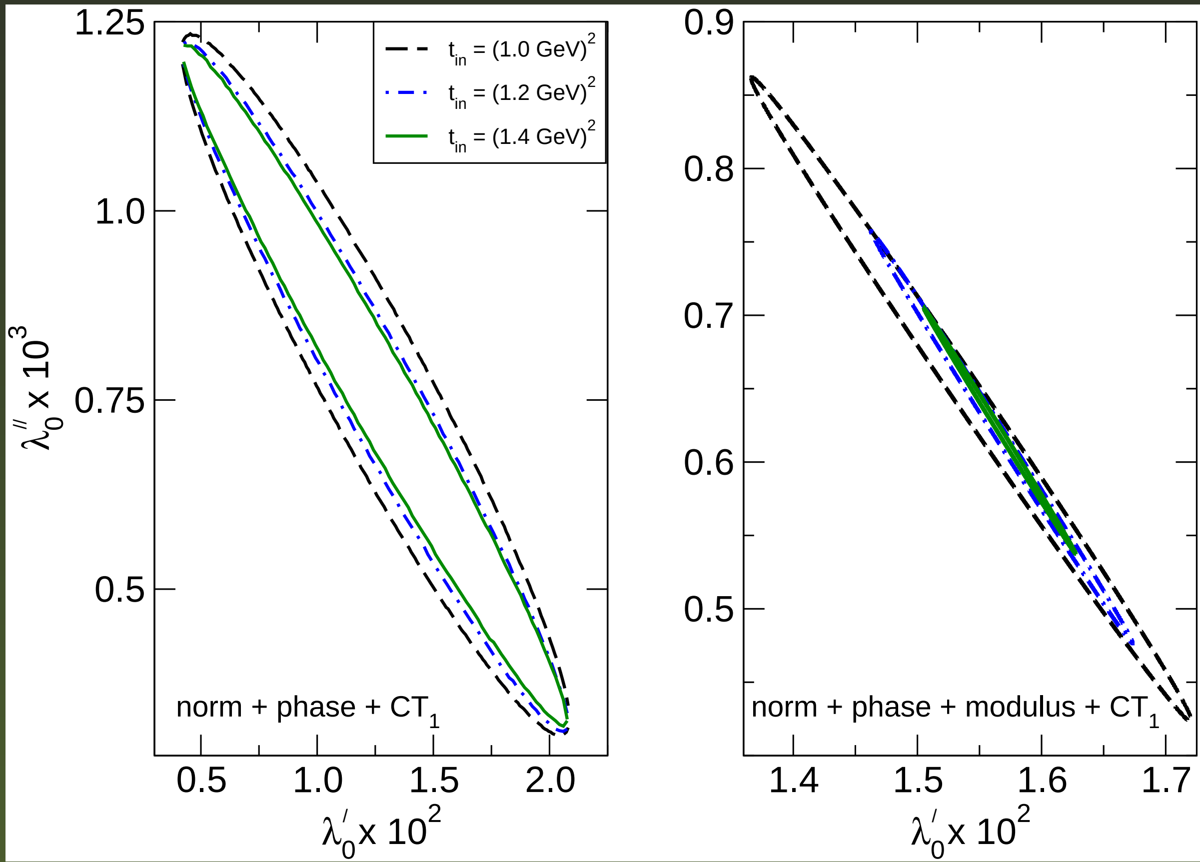

Comparison of Allowed regions with phase (and modulus) with different values of t_{in} and CT$_1$ and CT$_2$

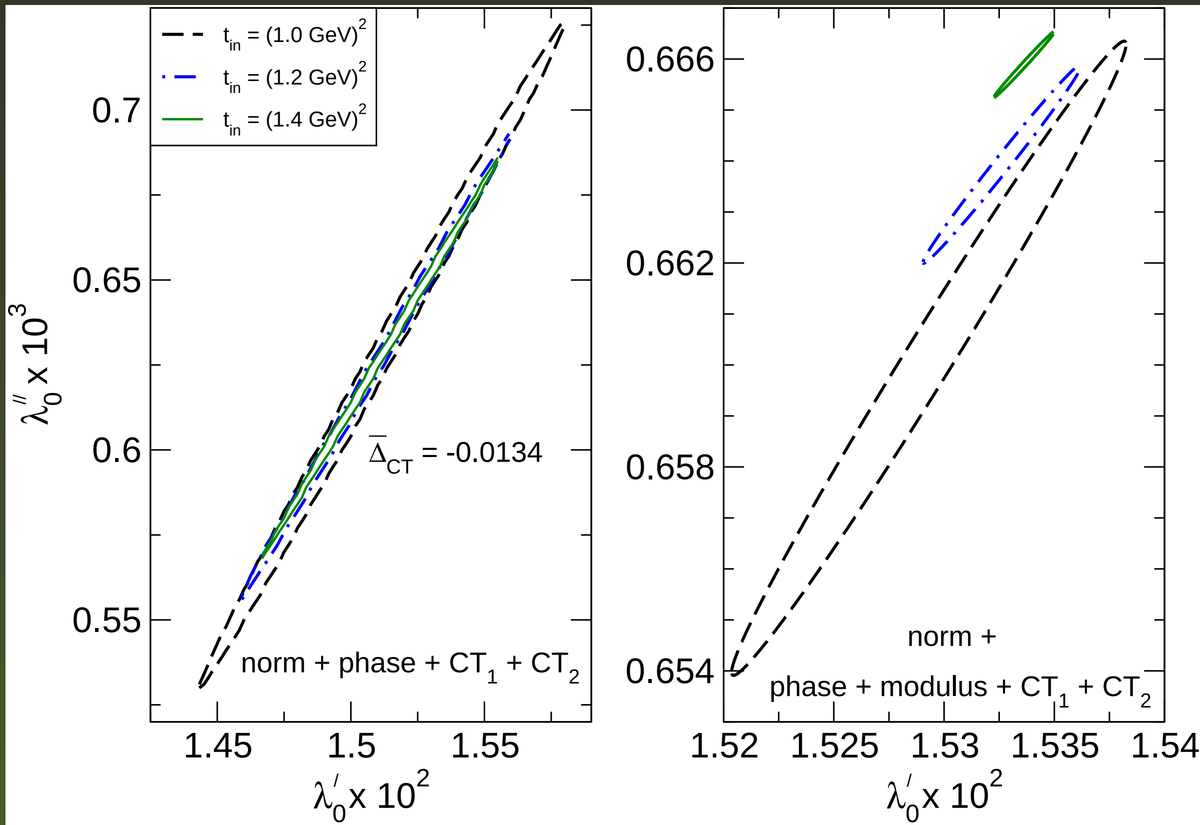

Results and conclusion

- We have reviewed the status of the vector and scalar form factors which are of fundamental importance to the standard model.

Results and conclusion

- We have reviewed the status of the vector and scalar form factors which are of fundamental importance to the standard model.
- We have introduced new methods to find stringent constraints using chiral symmetry, perturbative QCD, dispersion relations and unitarity

Results and conclusion

- We have reviewed the status of the vector and scalar form factors which are of fundamental importance to the standard model.
- We have introduced new methods to find stringent constraints using chiral symmetry, perturbative QCD, dispersion relations and unitarity
- The results are very stringent in the scalar form factor case.

Results and conclusion

- We have reviewed the status of the vector and scalar form factors which are of fundamental importance to the standard model.
- We have introduced new methods to find stringent constraints using chiral symmetry, perturbative QCD, dispersion relations and unitarity
- The results are very stringent in the scalar form factor case.
- Restricts the range of the slope to $\sim 0.01 - 0.02$, gives a near linear correlation with the curvature, restricts $\overline{\Delta}_{CT}$ to a small range

Results and conclusion

- We have reviewed the status of the vector and scalar form factors which are of fundamental importance to the standard model.
- We have introduced new methods to find stringent constraints using chiral symmetry, perturbative QCD, dispersion relations and unitarity
- The results are very stringent in the scalar form factor case.
- Restricts the range of the slope to $\sim 0.01 - 0.02$, gives a near linear correlation with the curvature, restricts $\overline{\Delta}_{CT}$ to a small range
- Tests the consistency of the determinations.